JOC Article

The Role of Hydrogen Bonds in Baeyer−Villiger Reactions

Shinichi Yamabe* and Shoko Yamazaki

Department of Chemistry, Nara University of Education, Takabatake-cho, Nara 630-8528, Japan

yamabes@nara-edu.ac.jp

Received December 26, 2006

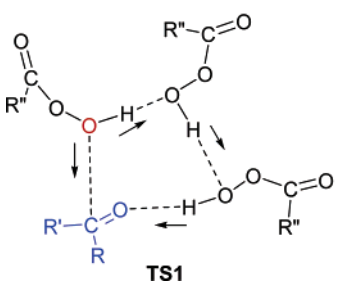

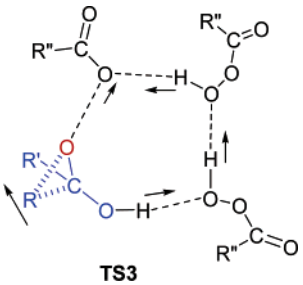

Various Baeyer−Villiger (B−V) oxidation reactions were examined by density functional theory calculations. Proton movements in transition states (TSs) of the two key steps, the nucleophilic addition of a peroxyacid molecule to a ketone (TS1) and the migration−cleavage of O−O (TS3), were discussed. A new TS of a hydrogen-bond rearrangement in the Criegee intermediate (TS2) was found. The hydrogen-bond directionality requires a trimer of the peroxyacid molecules at the nucleophilic addition of a peroxyacid molecule to a ketone TS (TS1). At the migration−cleavage of O−O TS (TS3), also three peroxyacid molecules are needed. Elementary processes of the B−V reaction were determined by the use of the (acetone and $(H-CO-OOH)_n$, $n = 3$) system. The geometries of the nucleophilic addition of a peroxyacid molecule to a ketone TS (TS1) and the migration−cleavage of O−O TS (TS3) in the trimer ($n = 3$) participating are nearly insensitive to the substituent on the peroxyacid. The directionality is satisfied in those geometries. The migration−cleavage of O−O TS (TS3) was found to be rate-determining in reactions, $[Me_2C{=}O + (H-CO-OOH)_3]$, $[Me_2C{=}O + (F_3C-CO-OOH)_3]$, and $[Me_2C{=}O + (MCPBA)_3]$. In contrast, the nucleophilic addition of a peroxyacid molecule to a ketone (TS1) is rate-determining in the reaction, $[Ph(Me)C{=}O + (H-CO-OOH)_3]$.

Introduction

The Baeyer−Villiger (B−V) oxidation is the oxidative cleavage of a carbon−carbon bond adjacent to a carbonyl, which converts ketones to esters and cyclic ketones to lactones (Scheme 1). The B−V oxidation can be carried out either with peroxyacids, such as $F_3C-CO-OOH$ and MCBPA (*meta*-chloroperbenzoic acid), or with hydrogen peroxide and a Lewis acid.[1]

The reaction is of great importance for the manufacture of lactones. The regiospecificity of the reaction depends on the relative migratory ability of the substituents attached to the carbonyl group. Substituents which are able to stabilize a positive charge migrate more readily, so that the order of preference is *tert*-alkyl > cyclohexyl > *sec*-alkyl > phenyl > *primary*-alkyl > CH_3. In some cases, stereoelectronic or ring strain factors also affect the regiochemical outcome. The reaction of aldehydes preferably gives formates, but sometimes only the liberated alcohol may be isolated due to the solvolytic instability of the product formate under the reaction conditions.[2]

SCHEME 1. Representative Baeyer−Villiger Oxidations

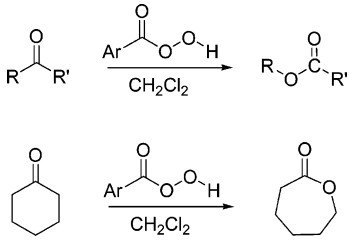

(1) (a) Baeyer, A.; Villiger, V. *Ber.* **1899**, *32*, 3625. (b) Baeyer, A.; Villiger, V. *Ber.* **1900**, *33*, 858. (c) House, H. O. *Modern Synthetic Reactions*, 2nd ed.; Benjamin: Menlo Park, CA, 1972; pp 306−307 and 321−328. (d) Krow, G. R. *Org. React.* **1993**, *43*, 251.

(2) (a) Smith, P. A. In *Molecular Rearrangements*; de Mayo, P., Ed.; Interscience: New York, 1963; Vol. 1. (b) Renz, M.; Meunier, B. *Eur. J. Org. Chem.* **1999**, 737.

10.1021/jo0626562 CCC: $37.00
Published on Web 03/17/2007

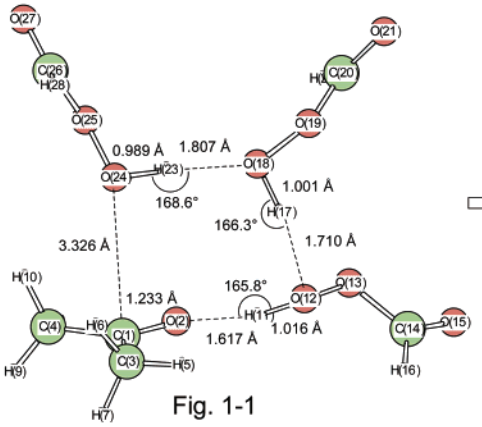

Fig. 1-1

ΔG° = 0 kcal/mol
(ΔG° = -1.97 kcal/mol), (ΔS° = -35.64 e.u.)
[ΔG° = 0 kcal/mol]

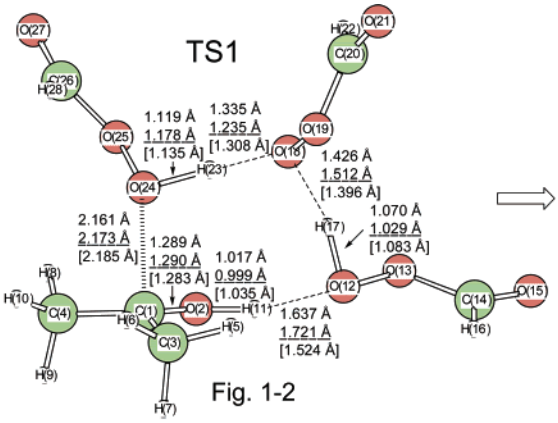

Fig. 1-2

ΔG‡ = +20.36 kcal/mol
(ΔG‡ = +18.39 kcal/mol), (ΔS‡ = -57.35 e.u.)
[ΔG‡ = +22.42 kcal/mol]

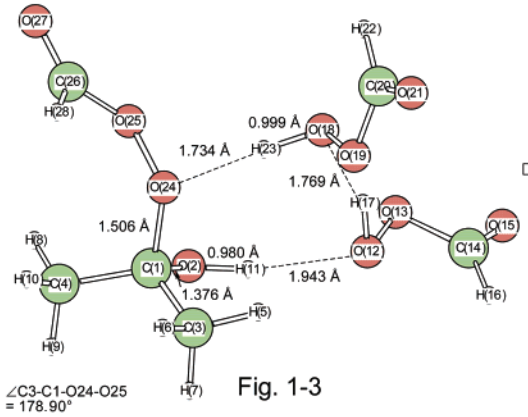

Fig. 1-3

ΔG° = +8.13 kcal/mol, (ΔS° = -53.38 e.u.)
[ΔG° = +11.92 kcal/mol]

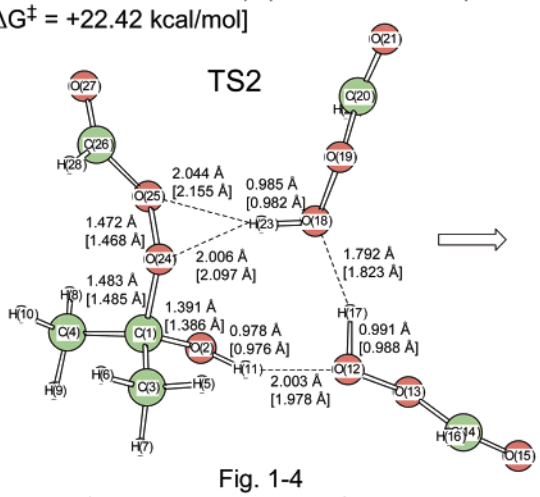

Fig. 1-4

ΔG‡ = +9.13 kcal/mol, (ΔS‡ = -55.88 e.u.)
[ΔG‡ = +12.88 kcal/mol]

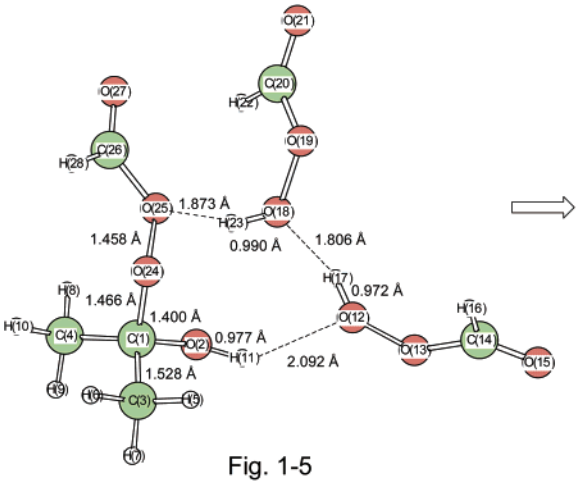

Fig. 1-5

ΔG° = +5.84 kcal/mo, (ΔS° = -52.37 e.u.)
[ΔG° = +8.70 kcal/mol]l

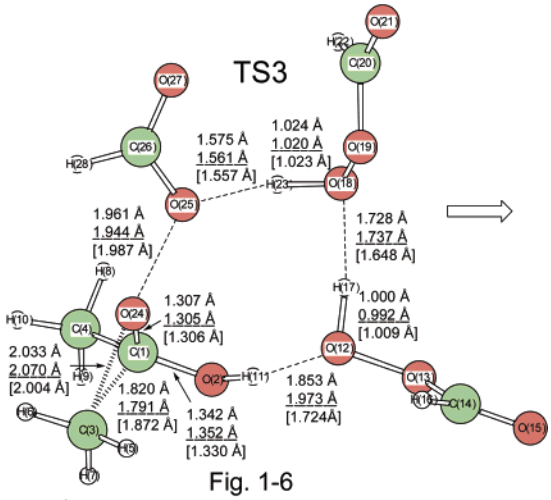

Fig. 1-6

ΔG‡ = +24.75 kcal/mol
(ΔG‡ = +22.78 kcal/mol), (ΔS‡ = -55.33 e.u.)
[ΔG‡ = +27.26 kcal/mol]

FIGURE 1. Reaction paths of acetone and (peroxyformic acid)$_3$ to methyl acetate, formic acid, and (peroxyformic acid)$_2$ (n = 3). Changes of the Gibbs free energies ($\Delta G°$ and $\Delta G^{\ddagger}$) were calculated by RB3LYP/6-31G* SCRF=dipole. Reaction coordinate vectors of TSs corresponding to respective imaginary frequencies ($\nu^{\ddagger}$) are shown in Figure S1 of Supporting Information. $\Delta G°$ values in parentheses are relative to the sum of $G°$(acetone) and $G°$((H−CO−OOH)$_3$). $\Delta S°$ values in parentheses are relative to the sum of $S°$(acetone) = 73.11 eu and $S°$((H−CO−OOH)$_3$) = 141.64 eu. The underlined numbers of TS1 (Figure 1-2) and TS (Figure 1-6) are the distances optimized by RB3LYP/6-311+G(d,p) SCRF=dipole. In the square brackets, RB3LYP/6-31++G** SCRF=dipole data are shown.

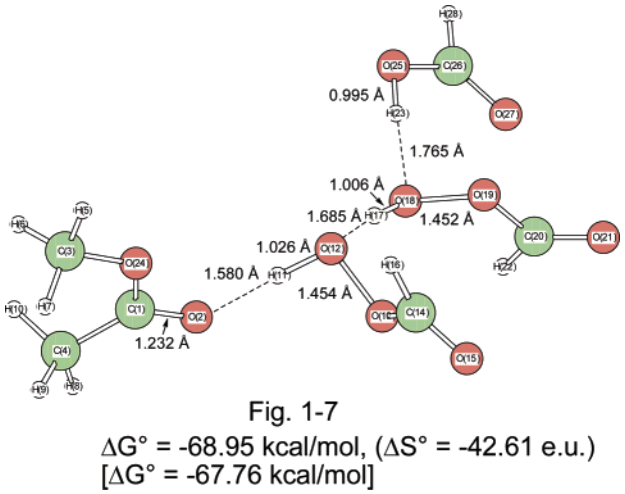

FIGURE 1. *Continued*

SCHEME 2. A Plausible Mechanism of the Baeyer−Villiger Oxidation[a]

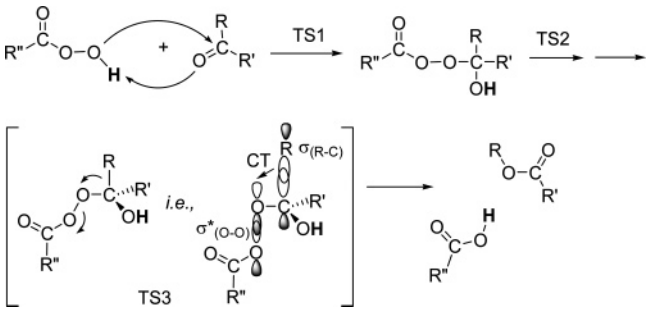

[a] The substituent R is the migrating group. TS denotes a transition state. At TS3, CT is the charge transfer interaction to regulate the R−C−O−O *trans* conformation. TS2 is an isomerization TS which will be shown in Figures 1-4 and 3-4.

The B−V reaction by the peroxyacid consists of the nucleophilic addition of the peroxide reagent to the carbonyl carbon of the substrate to afford the tetrahedral Criegee intermediate.[3] The intermediate undergoes intramolecular rearrangement of an alkyl or aryl substituent from the central carbon to the oxygen. The migration is accompanied by cleavage of the O−O bond and simultaneous formation of the ester (or lactone) and a carboxylic acid. At the migration step (TS3), the dihedral angle of R−C−O−O should be nearly 180° to maximize the σ(R−C)−σ*(O−O) overlap for the effective CT interaction (Scheme 2).[4]

The rate of the rearrangement is enhanced by the electron-withdrawing groups on the peroxyacid and peroxide because the σ*(O−O) energy level is lowered by the groups. The migration step (TS3) has been thought to be a rate-determining one in terms of the negative ρ value of the Hammett plot for the substituted acetophenones.[5] Also, the result of the isotope effect on the B−V reactions between acetophenones and MCPBA supported the rate-determining step.[6] However, several kinetic results have not been straightforwardly explicable, and the complex kinetics have been controversial.[7]

SCHEME 3. Molecular Models for TS1 Which Take into Account the Steric Conditions of the Orbital Interaction and the Proton Shift[a]

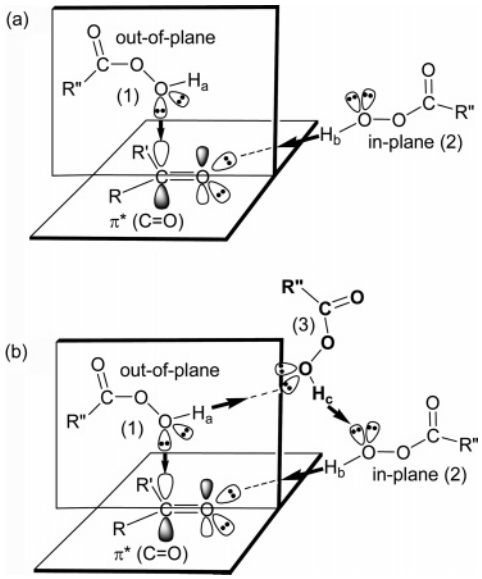

[a] The third peracid molecule (3) is needed to connect out-of-plane and in-plane molecules. Bold arrows indicate movement of specific atoms.

There have been various computational studies to elucidate the mechanism.[8] BF_3-,[8f] Sn-,[8g] and Ti[8h]-catalyzed B−V reactions with H_2O_2 were examined. Semiempirical (PM3 and AM1) MO calculations were made on model systems of (polymethoxybenzaldehydes + peroxysuccinic acid)[8b] and acetone and substituted peracids.[8c] The *anti*-periplanar group migration was shown to be more favorable than that in the gauche group in ionic reaction systems.[4a] Acetic acid or trifluoroacetic acid was added to the (benzaldehyde + peroxyacetic acid) reacting

(3) Criegee, R. *Justus Liebigs Ann. Chem.* **1948**, *560*, 127.
(4) (a) Snowden, M.; Bermudez, A.; Kelly, D. R.; Radkiewicz-Poutsma, J. L. *J. Org. Chem.* **2004**, *69*, 7148. (b) Goodman, R. M.; Kishi, Y. *J. Am. Chem. Soc.* **1998**, *120*, 9392.
(5) Hawthorne, M. F.; Emmons, W. D. *J. Am. Chem. Soc.* **1958**, *80*, 6398.
(6) Palmer, B. W.; Fry, A. *J. Am. Chem. Soc.* **1970**, *92*, 2580.
(7) (a) Hassall, C. H. *Org. React.* **1957**, *9*, 73. (b) Lee, S. B.; Uff, B. C. *Quart. Rev.* **1967**, *21*, 429. (c) Yukawa, Y.; Ando, T.; Token, K.; Kawada, M.; Kim, S. *Tetrahedron Lett.* **1969**, *28*, 2367. (d) Winnik, M. A.; Stoute, V.; Fitzgerald, P. *J. Am. Chem. Soc.* **1974**, *96*, 1977. (e) Friess, S. L.; Soloway, A. H. *J. Am. Chem. Soc.* **1951**, *73*, 3968. (f) Doering, W. E.; Speers, L. *J. Am. Chem. Soc.* **1950**, *72*, 5515. (g) Ogata, Y.; Sawaki, Y. *J. Org. Chem.* **1972**, *37*, 2953. (h) Ogata, Y.; Sawaki, Y. *J. Am. Chem. Soc.* **1972**, *94*, 4189. (i) Ogata, Y.; Sawaki, Y. *J. Org. Chem.* **1969**, *34*, 3985.

SCHEME 4. Molecular Models for TS3 Which Take into Account the Steric Conditions[a]

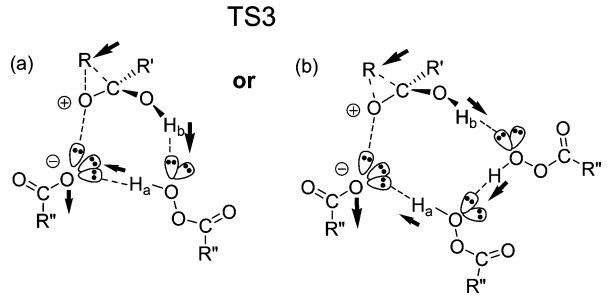

[a] To ensure the hydrogen-bond linearity, one (a) or two (b) auxiliary peracid molecules are necessary.

SCHEME 5. Alternative Models of TS1 and TS3[a]

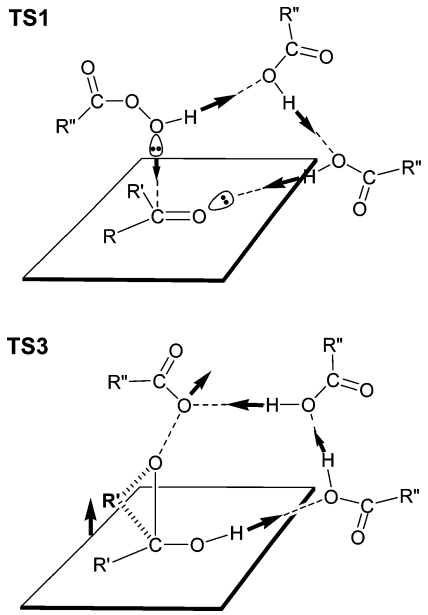

[a] The two peracid molecules are replaced with two carboxylic acids.

SCHEME 6. A Transition State (TS1) to Form the Criegee Intermediate Reported in Ref 14

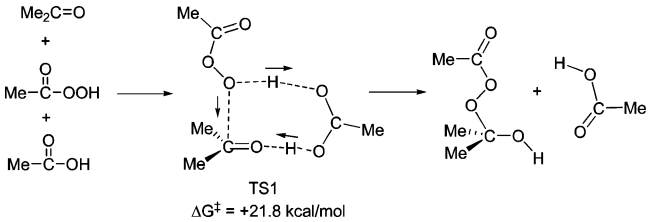

system, and the catalyst was found to lower the activation energy and changes the rate-determining step.[8e] Grein et al. reported that the first step (TS1) is the rate-determining step and that the energy of TS1 is 15−20 kcal/mol larger than that of TS2.[8i] This result seems to be inconsistent with the experimental evidence.[7] The four-center model would be inappropriate to describe the geometry of TS1.

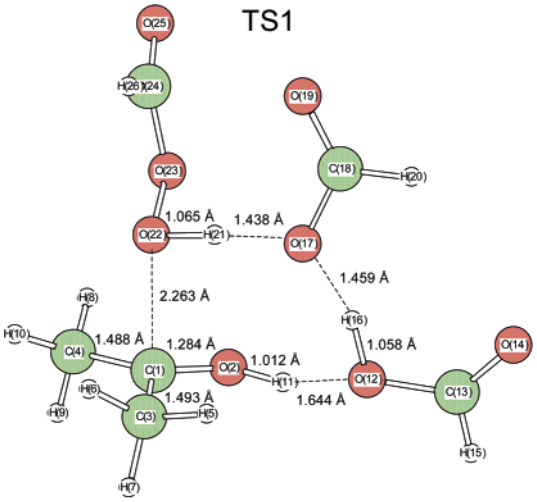

Fig. 2-1
ΔG‡ = +35.85 kcal/mol

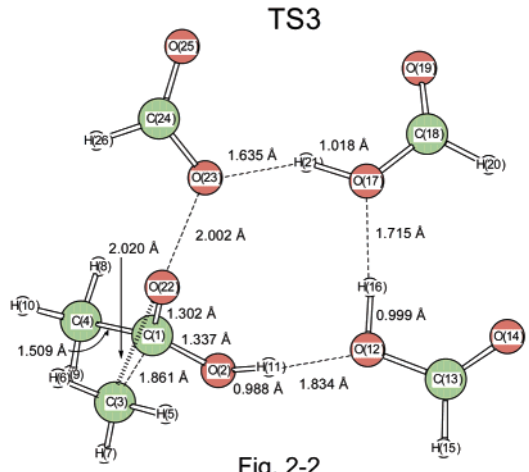

Fig. 2-2
ΔG‡ = +40.72 kcal/mol

FIGURE 2. TS1 and TS3 in a reaction of acetone, peroxyformic acid, and (formic acid)$_2$ to methyl acetate and (formic acid)$_3$. The reaction coordinate vectors of TS1 and TS3 are shown in Figure S4 of Supporting Information.

Despite these theoretical studies, the mechanism of the typical B−V reactions between ketones and peroxyacids is not yet settled. The most significant problem in Scheme 2 is a lack in the detailed motion of the proton shown by the bold symbol. The proton release and acceptance are caused by the interchange of O−H covalent and H···O hydrogen bonds. The interchange requires the O−H···O line, that is, the hydrogen-bond directionality. Scheme 2 should be revised, so that the proton movement satisfying the above requirement is involved.

In this work, the role of hydrogen bonds on the two steps (TS1 and TS3) in Scheme 2 was examined computationally and precisely. Various substrates and peroxyacids were employed to compare the B−V reactivities. Proton relays via the peroxyacid trimer were found to give plausible reaction paths.

(8) (a) Stoute, V. A.; Winnik, M. A.; Csizmadia, I. G. *J. Am. Chem. Soc.* **1974**, *96*, 6388. (b) Hannachia, H.; Anounea, N.; Arnauda, C.; Lanteria, P.; Longeraya, R.; Chermetteb, H. *J. Mol. Struct. (THEOCHEM)* **1998**, *434*, 183. (c) Cadenasa, R.; Reyes, L.; Lagunez-Oteroa, J.; Cetina, R. *J. Mol. Struct. (THEOCHEM)* **2000**, *497*, 211. (d) Cardenas, R.; Cetina, R.; Lagunez-Otero, J.; Reyes, L. *J. Phys. Chem. A* **1997**, *101*, 192. (e) Okuno, Y. *Chem.—Eur. J.* **1997**, *3*, 212. (f) Carlqvist, P.; Eklund, R.; Brinck, T. *J. Org. Chem.* **2001**, *66*, 1193. (g) Sever, R. R.; Root, T. W. *J. Phys. Chem. B* **2003**, *107*, 10521. (h) Sever, R. R.; Root, T. W. *J. Phys. Chem. B* **2003**, *107*, 10848. (i) Grein, F.; Chen, A. C.; Edwards, D.; Crudden, C. M. *J. Org. Chem.* **2006**, *71*, 861.

Method of Calculations

The geometries of reacting systems between ketones and peroxyacids were determined by density functional theory calculations. The ketones are acetone and acetophenone. The peracids are formic peroxyacid, trifluoro-peroxyacetic acid, and MCPBA. The B3LYP/6-31G* method[9] was used for geometry optimizations. B3LYP seems to be a suitable method because it includes the electron correlation effect to some extent. At the optimizations, the solvent effect was taken into account by Onsager's self consistent field[10] with the dielectric constant of 8.93 (CH_2Cl_2). All the geometries were also optimized with RB3LYP/6-31++G**. Further, for TS1 and TS3 of Figure 1, RB3LYP/6-311+G(d,p) geometry optimizations were carried out.

Transition states (TSs) were characterized by vibrational analyses, which checked whether the obtained geometries have single imaginary frequencies ($\nu^{\ddagger}$). From TSs, reaction paths were traced by the IRC (intrinsic reaction coordinate in the mass-weighted Cartesian coordinate) method[11] to obtain the energy-minimum geometries. $\Delta G°$ values without parentheses were calculated relative to the Gibbs free energy (T = 300 K) of the pre-reaction complex ("precursor", e.g., in Figure 1-1). Those with parentheses are relative to the sum of $G°$(acetone) and $G°$((peracid)$_n$). All the calculations were carried out using the Gaussian 03[12] program package at the Information Processing Center (Nara University of Education).

Molecular-Model Discussion of Catalyst-Free Reacting Systems

In Scheme 2, TS1 consists of the nucleophilic attack by the peroxyacid to the carbonyl carbon of the ketone substrate. The attack by the peracid (1) occurs out of plane as Scheme 3a shows.

At the same time, a proton is migrated from the peroxyacid (2) to the in-plane lone-pair orbital. Thus, formation of the C−O bond and that of the O−H_b one takes place perpendicularly and independently. Formally, the resultant adduct between the peroxyacid (1) and the ketone is a cation, and the peroxyacid (2) is a conjugate base (anion) after the proton H_b is lost. To retain the neutral reaction condition, one more peroxyacid molecule (3) is needed. The third molecule may capture H_a and may release a proton, H_c. Participation of the trimer in TS1 may give ready bond interchanges. In fact, in our previous work,[13] a tetrahedral intermediate was found to be formed by the water-trimer reactant for hydrolysis of ethyl acetate.

At TS3 of Scheme 2, formally, the proton (bold symbol) is shifted toward the dissociating carboxylate, R″−COO−. However, the direct shift is obviously unlikely according to the hydrogen-bond linearity. Scheme 4 shows that one (a) or two (b) peroxyacid molecule(s) is concerned with the proton relays at TS3.

Calculations are necessary to judge which (a or b) is more favorable. Since TS1 (Scheme 3) requires definitely the peroxyacid trimer, TS3 will be first traced by the use of the trimer computationally. Second, reaction models with the dimer and tetramer will be also examined.

Results of Calculations and Discussions

Reactions of Acetone, Peroxyformic Acid, and Formic Acid Molecules. Figure 1 shows the reaction path of $Me_2C{=}O + (H{-}CO{-}OOH)_3 \rightarrow Me{-}CO{-}OMe + H{-}CO{-}OH + (H{-}CO{-}OOH)_2$. Figure 1-1 exhibits the precursor geometry which is in line with that in Scheme 3b. The first H−CO−OOH molecule (1) is coordinated out-of-plane to the carbonyl carbon. The second molecule (2) is in-plane to the lone-pair orbital of the carbonyl oxygen atom. The third molecule (3) connects 1 with 2. Three hydrogen-bond angles are 168.6, 166.3, and 165.8°, which satisfy nearly the hydrogen-bond linearity. In the assumed equilibrium, acetone + $(H{-}CO{-}OOH)_3 \rightleftarrows$ the precursor (Figure 1-1), the relative free energy is −1.97 kcal/mol (in the parentheses). Usually, the association leads to $\Delta G° > 0$ because of the entropy loss, $\Delta S° < 0$. In fact, a large negative value $\Delta S° = -35.64$ cal/(mol·K) was obtained for the precursor (Figure 1-1). Despite the large entropy loss, the negative $\Delta G°$ value demonstrates that the trimer association is likely to stabilize the reacting system. Figure 1-2 shows the geometry of TS1. Owing to the strainless hydrogen-bond circuit, bond interchanges and proton relays occur simultaneously. After TS1, the Criegee intermediate linked with the H−CO−OOH dimer was obtained (Figure 1-3). The dihedral angle, C3−C1−O24−O25 = 178.90°, is consistent with the *trans* conformation controlled by the σ(R−C)−σ^*(O−O) CT interaction (Scheme 2). The interaction also compels a small bond angle of C3−C1−O24, 100.6° (normally 109.5°), which shows the incipient Me migration. In the geometry of Figure 1-3, there is a hydrogen bond, O24···H23, which is originally a covalent bond in Figure 1-1. To convert the O27H28C26O25 moiety to a formic acid, the proton H23 needs to be hydrogen bonded to O25. The hydrogen-bond switch TS (TS2) is shown in Figure 1-4. After TS2, the second Criegee intermediate is formed and is exhibited in Figure 1-5. It is slightly more stable than the first one (ΔG = +8.13 kcal/mol in Figure 1-3 and ΔG = +5.84 kcal/mol in Figure 1-5). From the second intermediate, TS3 is brought about (Figure 1-6). Migration of the methyl (C3H5H6H7) group, cleavage of the O24−O25 bond, and interchanges of (O25···H23−O18 → O25−H23···O18), (O18···H17−O12 → O18−H17···O12), and (O12···H11−O2 → O12−H11···O2) occur simultaneously. The H−CO−OOH dimer is fit conformationally for the proton acceptance and release. After TS3, the product (methyl acetate, formic acid, and dimer of H−CO−OOH) is reached (Figure 1-7). In Figure 1, the rate-determining step is TS3 with $\Delta G^{\ddagger}$ = +24.75 kcal/mol. All the geometries in Figure 1 are in accord with those predicted in Schemes 3b and 4b.

RB3LYP/6-31++G** results are shown in square brackets. Their ΔG values are a few kcal/mol larger than RB3LYP/6-31G* values, which comes probably from the greater stabilization of the reactant (Figure 1-1) by RB3LYP/6-31++G*.

(9) (a) Becke, A. D. *J. Chem. Phys.* **1993**, *98*, 5648. (b) Lee, C.; Yang, W.; Parr, R. G. *Phys. Rev. B* **1998**, *37*, 785.

(10) Onsager, L. *J. Am. Chem. Soc.* **1936**, *58*, 1486.

(11) (a) Fukui, K. *J. Phys. Chem.* **1970**, *74*, 4161. (b) Gonzalez, C.; Schlegel, H. B. *J. Phys. Chem.* **1987**, *90*, 2154.

(12) Frisch, M. J.; Trucks, G. W.; Schlegel, H. B.; Scuseria, G. E.; Robb, M. A.; Cheeseman, J. R.; Montgomery, J. A., Jr.; Vreven, T.; Kudin, K. N.; Burant, J. C.; Millam, J. M.; Iyengar, S. S.; Tomasi, J.; Barone, V.; Mennucci, B.; Cossi, M.; Scalmani, G.; Rega, N.; Petersson, G. A.; Nakatsuji, H.; Hada, M.; Ehara, M.; Toyota, K.; Fukuda, R.; Hasegawa, J.; Ishida, M.; Nakajima, T.; Honda, Y.; Kitao, O.; Nakai, H.; Klene, M.; Li, X.; Knox, J. E.; Hratchian, H. P.; Cross, J. B.; Adamo, C.; Jaramillo, J.; Gomperts, R.; Stratmann, R. E.; Yazyev, O.; Austin, A. J.; Cammi, R.; Pomelli, C.; Ochterski, J. W.; Ayala, P. Y.; Morokuma, K.; Voth, G. A.; Salvador, P.; Dannenberg, J. J.; Zakrzewski, V. G.; Dapprich, S.; Daniels, A. D.; Strain, M. C.; Farkas, O.; Malick, D. K.; Rabuck, A. D.; Raghavachari, K.; Foresman, J. B.; Ortiz, J. V.; Cui, Q.; Baboul, A. G.; Clifford, S.; Cioslowski, J.; Stefanov, B. B.; Liu, G.; Liashenko, A.; Piskorz, P.; Komaromi, I.; Martin, R. L.; Fox, D. J.; Keith, T.; Al-Laham, M. A.; Peng, C. Y.; Nanayakkara, A.; Challacombe, M.; Gill, P. M. W.; Johnson, B.; Chen, W.; Wong, M. W.; Gonzalez, C.; Pople, J. A. *Gaussian 03*, revision C.02; Gaussian Inc.: Wallingford, CT, 2004.

(13) Yamabe, S.; Tsuchida, N.; Hayashida, Y. *J. Phys. Chem. A* **2005**, *109*, 7216.

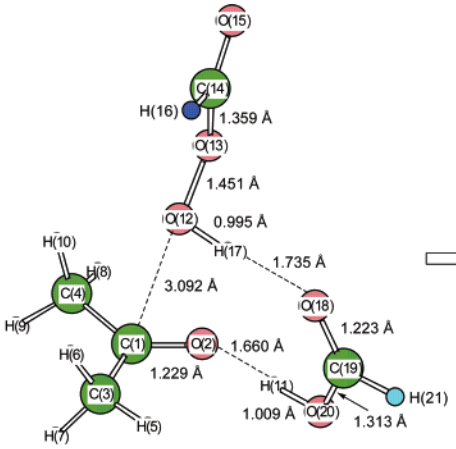

Fig. 3-1
ΔG° = 0 kcal/mol
<ΔG° = 0 kcal/mol>
<<ΔG° = 0 kcal/mol>>

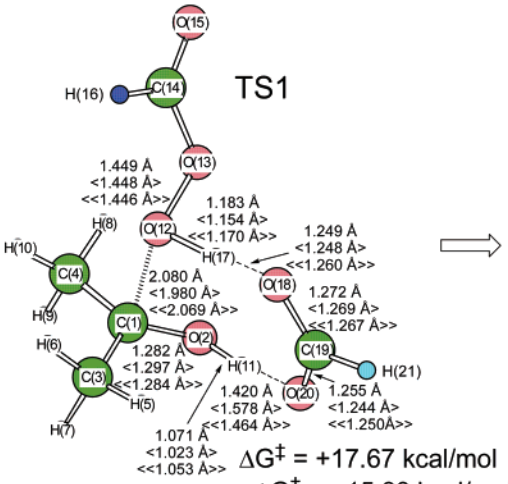

Fig. 3-2
ΔG‡ = +17.67 kcal/mol
<ΔG‡ = +15.88 kcal/mol>
<<ΔG‡ = +15.56 kcal/mol>>

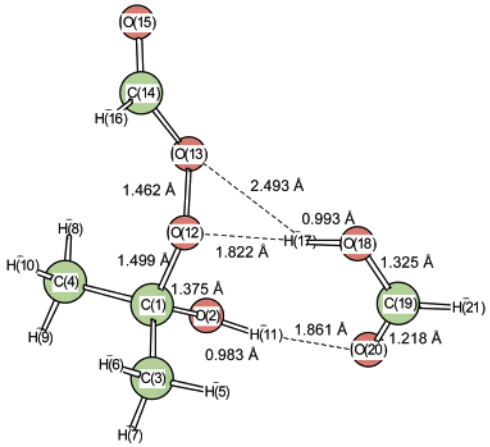

Fig. 3-3
ΔG° = +6.80 kcal/mol

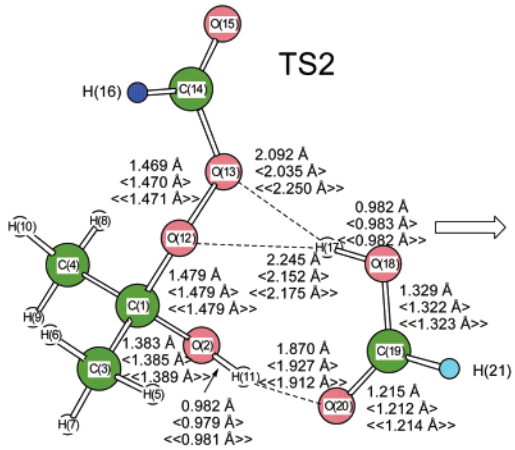

Fig. 3-4
ΔG‡ = +8.35 kcal/mol
<ΔG‡ = +9.75 kcal/mol>
<<ΔG‡ = +9.41 kcal/mol>>

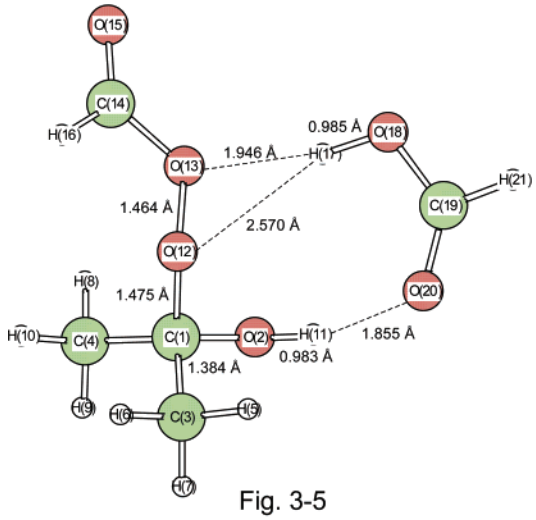

Fig. 3-5
ΔG° = +7.16 kcal/mol

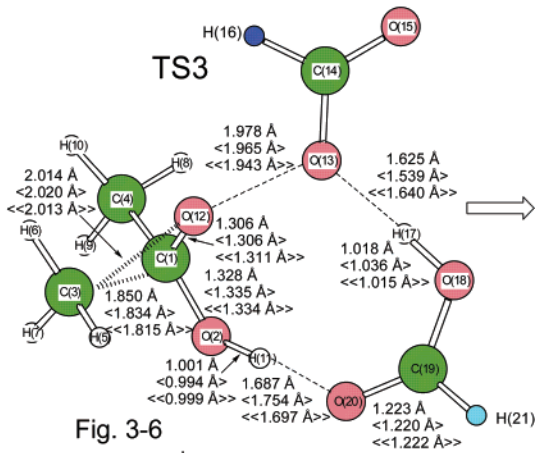

Fig. 3-6
ΔG‡ = +26.95 kcal/mol
<ΔG‡ = +26.72 kcal/mol>
<<ΔG‡ = +20.61 kcal/mol>>

FIGURE 3. Reaction paths of acetone, formic acid, and peroxyformic acid to methyl acetate and $(\text{formic acid})_2$. Reaction coordinate vectors are shown in Figure S5 of Supporting Information. Geometries and free-energy changes for a reaction of acetone, trifluoroacetic acid, and peroxyformic acid are shown in braces < >, where H21 is substituted to the F_3C group. Results for a reaction of acetone, trifluoroacetic acid, and peroxytrifluoroacetic acid are shown in double braces ≪ ≫, where H21 and H16 are substituted to F_3C groups.

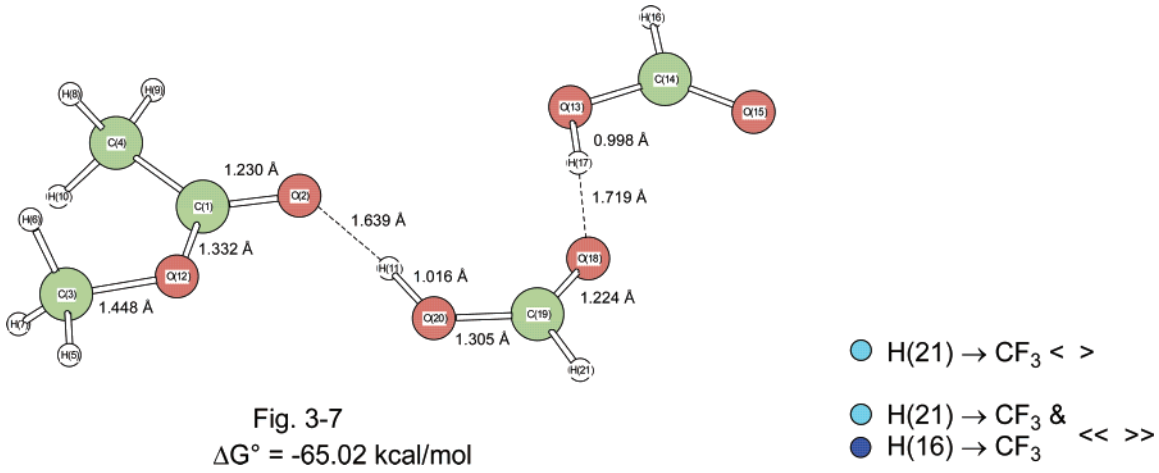

FIGURE 3. *Continued*

However, the relative energies (i.e., $\Delta\Delta G$ values) are found to be almost the same. TS geometries by RB3LYP/6-31G*, RB3LYP/6-311+G(d,p), and RB3LYP/6-31++G(d,p) are similar.

The possibility of the peracid trimer association was examined in terms of the change of free energies. The $\Delta G°$ values for the equilibrium, monomer + monomer ⇄ dimer, is +3.99 kcal/mol. The value for monomer + dimer ⇄ trimer is +3.37 kcal/mol. The corresponding equilibrium constant for monomer + dimer ⇄ trimer is $K = 3.52 \times 10^{-3}$ *l*/mol ($T = 300$ K) according to the van't Hoff equation. Thus, although the concentration of the trimer itself is small, the association in Figure 1-1 may shift the equilibrium toward the trimer according to the Le Chatelier's law.

The dimer ($n = 2$) or tetramer ($n = 4$) of $(H-CO-OOH)_n$ might be a reactant toward the acetone. Figure S2 in the Supporting Information shows two transition states of $n = 2$. $\Delta G^‡$ (TS1, $n = 2$) = +30.08 kcal/mol is larger than $\Delta G^‡$ (TS1, $n = 3$) = +20.36 kcal/mol in Figure 1-2. $\Delta G^‡$ (TS3, $n = 2$) = +31.02 kcal/mol is also larger than $\Delta G^‡$ (TS3, $n = 3$) = +24.75 kcal/mol in Figure 1-6. The $n = 2$ reaction is less favorable than the $n = 3$ reaction energetically. In TS1 (Figure S2-1), the angle ∠O2−H11−O12 is 146.12°. This nonlinear linkage makes TS1 of $n = 2$ unfavorable. The need of the conformation in Scheme 3b, that is, $n = 3$, is confirmed. In TS3 (Figure S2-2), the angle ∠O2−H11···O17 is 153.91°. This nonlinear linkage makes TS3 of $n = 2$ unfavorable again. The superiority of b over a in Scheme 4 is confirmed.

The $n = 4$ reaction was examined. Figure S3 in the Supporting Information exhibits TS1 and the resultant Criegee intermediate of $n = 4$. $\Delta G^‡$ (TS1, $n = 4$) is 22.80 kcal/mol and is slightly larger than $\Delta G^‡$ (TS1, $n = 3$) = 20.36 kcal/mol in Figure 1-2. TS3 of $n = 4$ could not be obtained, which can be understood by the geometry of the Criegee intermediate. In the geometry (Figure S3-2), the dihedral angle of C3−C1−O29−O31 is −57.50°. This angle does not correspond to the *trans* conformation needed for the Me migration in Scheme 2. Steric crowd reinforces the dihedral angle. Accordingly, the bond angle ∠C3−C1−O29 = 108.70° is normal and does not show the incipient migration. Besides the specific unfavorable geometric condition, $n = 4$ is unlikely entropically. Thus, the trimer participation in the B−V reaction is found to be best.

In Schemes 3b and 4b, hydroxyl groups of two peroxyacid molecules work merely as proton donor and acceptor. Then, they might be replaced by carboxylic acid molecules (Scheme 5). The carboxylic acid is the product of the B−V reaction, and its concentration grows large as the reaction proceeds. Figure 2 shows two TS geometries. The activation free energies, ΔG (TS1) = +35.85 kcal/mol and $\Delta G^‡$ (TS3) = +40.72 kcal/mol, were obtained. They are substantially larger than $\Delta G^‡$ (TS1) = +20.36 kcal/mol and $\Delta G^‡$ (TS3) = 24.75 kcal/mol (Figure 1), respectively. The reaction model which involves two carboxylic acids but makes their carbonyl groups unconcerned with bond interchanges is unlikely owing to the rigid geometry of the carboxyl group.

Proton relays depicted in Schemes 3b, 4b, and 5 require the flexible reorientation of hydroxyl groups. As a free molecule, the formic acid with a dihedral angle 90° fixed (compulsively fixed out-of-plane) is +11.80 kcal/mol less stable than that in the equilibrium geometry. In contrast, the peroxyformic acid with the H−O−O−C dihedral angle, −124.9°, undergoes only +0.18 kcal/mol destabilization by the similar 90° compulsory twist. The peroxyformic acid molecules may adjust flexibly three-dimensional proton relays.

Recently, TS1 composed of acetone, peracetic acid, and acetic acid has been reported (Scheme 6).[14] Although a small activation energy, $\Delta G^‡$ = 21.8 kcal/mol, was obtained for TS1, TS3 has not been obtained yet. The entire process for the system of $Me_2C{=}O + H-CO-OOH + H-CO-OH$ has been determined and is shown in Figure 3. As found in ref 14, TS1 in Figure 3-2 has a very small energy, $\Delta G^‡$ = 17.67 kcal/mol, and the carboxylic acid participation in Scheme 6 promotes formation of the Criegee intermediate. On the other hand, TS3 in Figure 3-6 has a larger energy, $\Delta G^‡$ = 26.95 kcal/mol, than that in Figure 1-6, $\Delta G^‡$ = 24.75 kcal/mol. Thus, the autocatalytic role of carboxylic acids in the B−V reaction may be limited to TS1. In the Criegee intermediates, rearrangement of the hydrogen-bonded catalytic molecules would be likely in the middle or later stage of the B−V reaction.

The energy changes in the reaction of (acetone + H−CO−OOH + F_3CO-OH) and in that of (acetone + $F_3C-CO-OOH$ + F_3CO-OH) are shown in braces < > and double braces ≪ ≫, respectively. By the substitution of H(21) → F_3C, $\Delta G^‡$ (TS1) is decreased, +17.67 kcal/mol → <15.88 kcal/mol>; however, $\Delta G^‡$ (TS3) is almost the same, +26.95 kcal/mol ≃ <26.72 kcal/mol>. By the substitution of H(21) → F_3C and H(16) → F_3C,

(14) Alvarez-Idaboy, J. R.; Reyes, L.; Cruz, J. *Org. Lett.* **2006**, *8*, 1763.

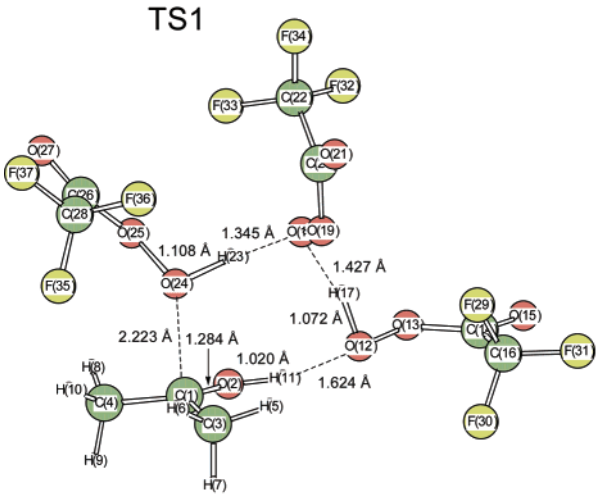

Fig. 4-1
$\Delta G^{\ddagger}$ = +17.49 kcal/mol

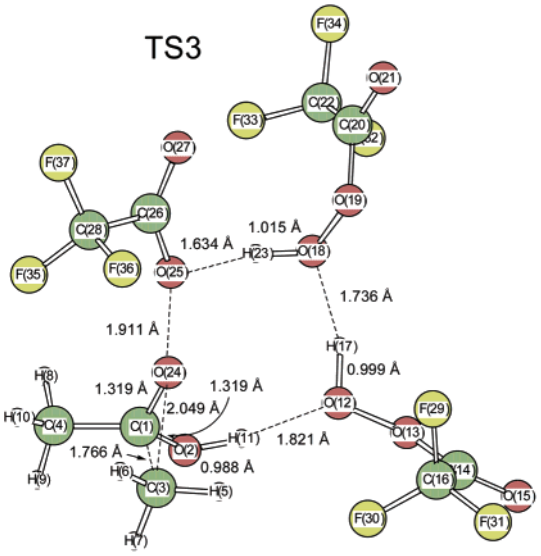

Fig. 4-2
$\Delta G^{\ddagger}$ = +19.00 kcal/mol

FIGURE 4. TS1 and TS3 in a reaction of acetone and (peroxy-trifluoroacetic acid)$_3$ to methyl acetate, trifluoroacetic acid, and (peroxy-trifluoroacetic acid)$_2$ (n = 3). The reaction coordinate vectors of TS1 and TS3 are shown in Figure S6 of Supporting Information.

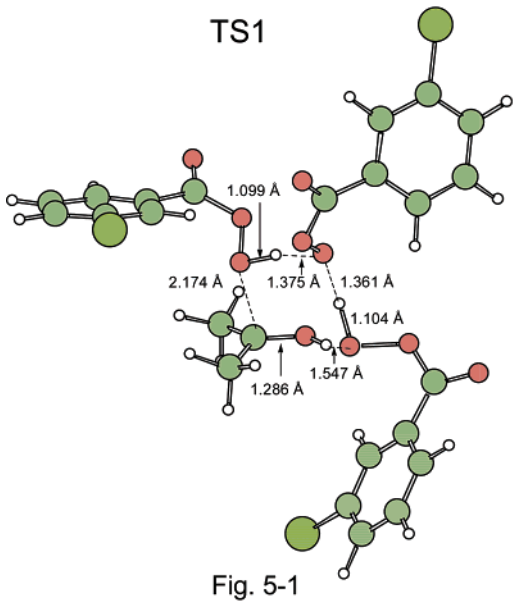

Fig. 5-1
$\Delta G^{\ddagger}$ = +21.63 kcal/mol
$\nu^{\ddagger}$ = 275.77i cm^{-1}

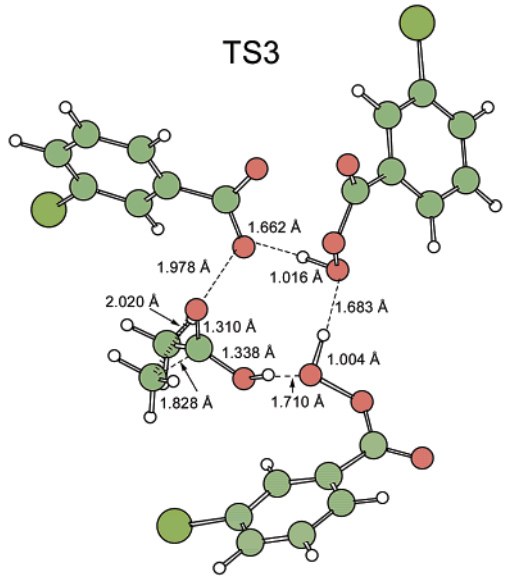

Fig. 5-2
$\Delta G^{\ddagger}$ = +25.88 kcal/mol
$\nu^{\ddagger}$ = 443.44i cm^{-1}

FIGURE 5. TS1 and TS3 in a reaction of acetone and (MCPBA)$_3$ to methyl acetate, *meta*-chlorobenzoic acid, and (MCPBA)$_2$ (n = 3). The reaction coordinate vectors could not be obtained due to the too large size of the reacting system for our drawing software.

$\Delta G^{\ddagger}$ (TS3) is decreased considerably, +26.95 kcal/mol → ≪20.61 kcal/mol≫. This energy change will be compared to that in Figure 4-2.

Reactions of Acetone and Other Peroxyformic Acids. In the previous subsection, participation of the trimer of peroxy-acids in the B−V reaction has been shown. Although the catalytic role of the carboxylic acid on TS1 has been confirmed in Figure 3, the acid is the product of the B−V reaction and is not contained in its initial stage. The initial, that is, catalyst-free stage, will be investigated further in this subsection. Two typical peroxyacids, peroxy-trifluoroacetic acid and MCPBA, are employed here. Since the elementary processes have been exhibited in Figure 1, two key steps (TS1 and TS3) will be presented hereafter. Figure 4 shows the geometries of TS1 and TS3 for $Me_2C{=}O$ and $(F_3C{-}CO{-}OOH)_3$. They are close to those in Figure 1 (i.e., $Me_2C{=}O$ and $(H{-}CO{-}OOH)_3$, respectively). However, the activation free energies, $\Delta G^{\ddagger}$ (TS1) = +17.49 kcal/mol and $\Delta G^{\ddagger}$ (TS3) = +19.00 kcal/mol, are much smaller than those of Figure 1. $\Delta G^{\ddagger}$ (TS1) = +17.49 kcal/mol is slightly larger than ≪$\Delta G^{\ddagger}$ (TS1) = +15.56 kcal/mol≫ of acetone + $F_3C{-}CO{-}OOH$ + $F_3C{-}CO{-}OH$ in Figure 3-2. In another respect, the catalytic role of the ketone, $F_3C{-}CO{-}OH$, is small relative to the uncatalyzed n = 3 reactivity. More noteworthy is that $\Delta G^{\ddagger}$ (TS3) = +19.00 kcal/mol in Figure 4-2 is smaller than ≪$\Delta G^{\ddagger}$ (TS3) = +20.61 kcal/mol≫ in Figure 3-6. The very high reactivity of $(F_3C{-}CO{-}OOH)_3$ is confirmed.

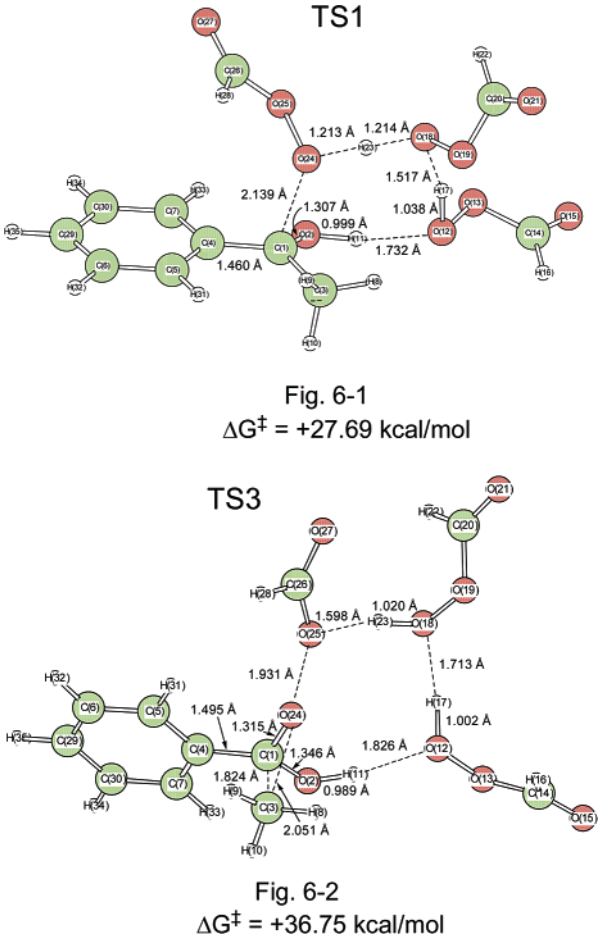

FIGURE 6. TS1 and TS3 in a reaction of acetophenone and (peroxyformic acid)$_3$ to phenyl acetate, formic acid, and (peroxyformic acid)$_2$ (n = 3). TS3 is for the methyl migration. The reaction coordinate vectors of TS1 and TS3 are shown in Figure S7 of Supporting Information.

TS3 is barely the rate-determining step. Bulky F_3C groups do not interfere with the circuit reaction region.

Figure 5 shows two TSs of acetone and (MCPBA)$_3$. Their geometries are also similar to those in Figures 1 and 4. Three *meta*-chlorobenzoyl groups are distant from the reaction region. In particular, they are remote from the migrating Me group. Therefore, even the larger size group may migrate without steric crowd. The free activation energies of TS1 and TS3 are slightly larger than those in Figure 1, which is a small discrepancy of the experimental reactivity order, MCPBA > H−CO−OOH. Probably, TSs containing MCPBA molecules would be subject to extra stabilization by the external solvent field (e.g., dispersion force).

Reactions of Acetophenone and Peroxyformic Molecules. The acetophenone substrate is considered here. Figure 6 shows two TSs for the Me group migration, which should be unfavorable in view of the order of the migratory ability raised in the Introduction. In fact, free activation energies, $\Delta G^{\ddagger}$ (TS1) = +27.69 kcal/mol and $\Delta G^{\ddagger}$ (TS3) = +36.75 kcal/mol, are larger than those in Figure 1. Figure 7 exhibits two TSs for the Ph migration. TS1 in Figure 7 is practically the same as that in Figure 6, and their free activation energies are almost the same. At TS3 of Figure 7, the C1−C3 distance is very short, 1.584 Å. If the C1−C3 bond were not broken at TS3, the bridged-

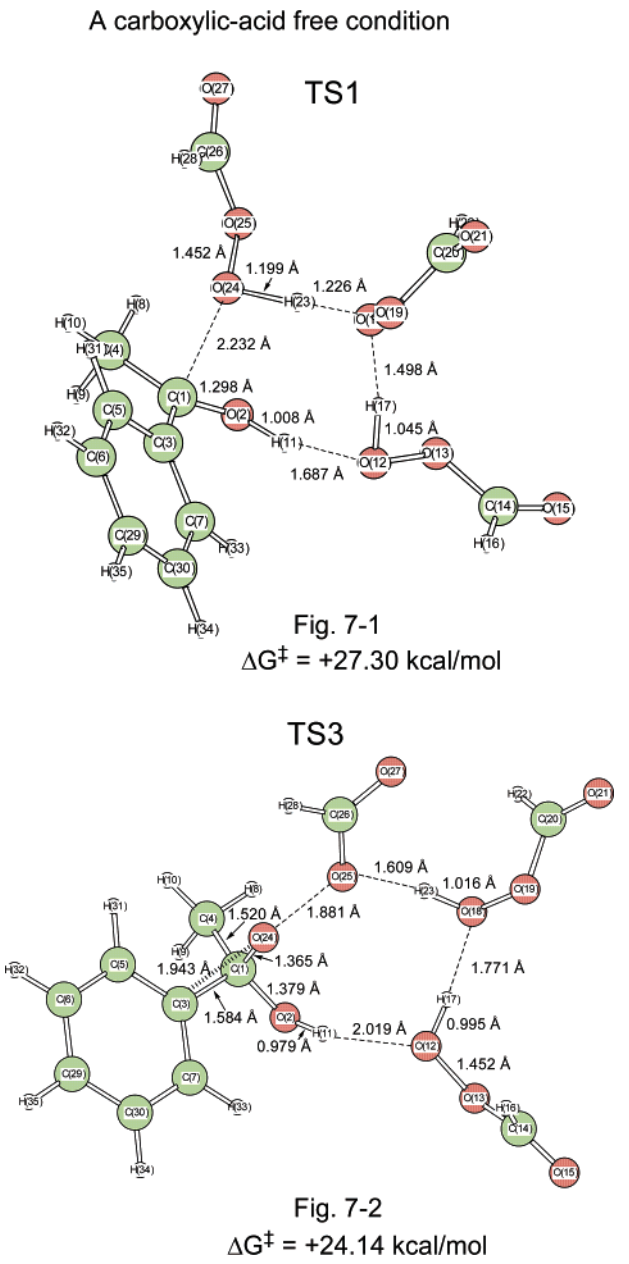

FIGURE 7. TS1 and TS3 in a reaction of acetophenone and (peroxyformic acid)$_3$ to methyl benzoate, formic acid, and (peroxyformic acid)$_2$ (n = 3). TS3 is for the phenyl migration. The reaction coordinate vectors of TS1 and TS3 are shown in Figure S8 of Supporting Information.

form (i.e., Cram's phenonium ion)[15] intermediate should be present. The IRC calculations[11] from TS3 were made, and at the forward point #113, a protonated ester-like geometry is formed. That is, the phenonium ion is not present after TS3. Noteworthy are free activation energies, $\Delta G^{\ddagger}$ (TS1) = 27.30 kcal/mol and $\Delta G^{\ddagger}$ (TS3) = 24.14 kcal/mol. TS1 is the rate-determining step, which is in contrast with the obtained trend in the other reactions (Figures 1−6). At TS1, the conjugation between the carbonyl and phenyl groups in the acetophenone substrate is broken, and to TS3, the phenonium-ion-like stability is added. These two factors would make TS1 the rate-determining step. However, the difference of the two free

(15) Cram, D. J. *J. Am. Chem. Soc.* **1964**, *86*, 3767.

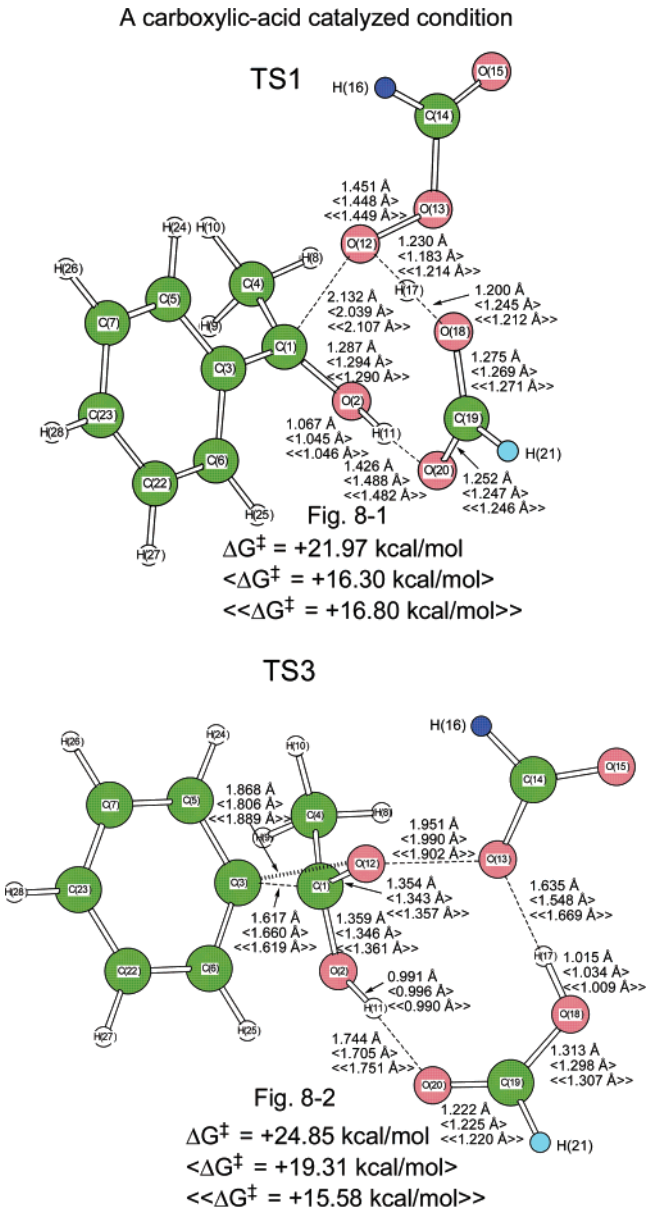

FIGURE 8. TS1 and TS3 in a reaction of acetophenone, peroxyformic acid, and formic acid to methyl benzoate and (formic acid)$_2$. TS3 is for the phenyl migration. The reaction coordinate vectors of TS1 and TS3 are shown in Figure S9 of Supporting Information. Values in braces < > are calculated for a reaction, acetophenone + H−CO−OOH + F_3C−CO−OH, where H21 is substituted to the F_3C group. Those in double braces ≪ ≫ are for acetophenone + F_3C−CO−OOH + F_3C−CO−OH, where H21 and H16 are substituted to F_3C groups.

activation energies are not large [27.30 (TS1) − 24.14 (TS3) = 3.16 kcal/mol)] and are critical. Thus, the present calculated result would be consistent with the postulate that "in the B−V reaction several steps can be rate-determining depending on the reaction conditions and the substrate itself".[2b] Palmer and Fry reported a rate constant of the second-order (4.53×10^{-3} L mol^{-1} s^{-1}) at 32 °C in $CHCl_3$ for the B−V reaction between acetophenone and MCPBA.[6] The constant corresponds to $\Delta G^{\ddagger}$ = +23.09 kcal/mol.[16] This experimental value is slightly smaller than the present $\Delta G^{\ddagger}$ (TS1) = +27.30 kcal/mol in Figure 7. Aside from the slight energy difference, the standard B−V reaction is thought to proceed readily in the neutral condition, that is, even without acid catalysts.

The process for the system of acetophenone + H−CO−OOH + H−CO−OH, analogous to Figure 3, was also determined and is shown in Figure 8. A result similar to that in Figure 3 was obtained, $\Delta G^{\ddagger}$ (Figure 7-1) > $\Delta G^{\ddagger}$ (Figure 8-1) for TS1 but $\Delta G^{\ddagger}$ (Figure 7-2) ≲ $\Delta G^{\ddagger}$ (Figure 8-2) for TS3. Thus, the autocatalytic role of carboxylic acids in the B−V reaction may be only effective in TS1 for acetophenone as well. The CF_3 substitution lowers $\Delta G^{\ddagger}$ values appreciably as shown in < > and ≪ ≫ values.

Concluding Remarks

In this work, various B−V reactions were examined computationally. Proton movements in the two key steps, the nucleophilic addition (TS1) and the migration−cleavage of O−O (TS3), were discussed in Schemes 3 and 4 according to the criterion of the hydrogen-bond directionality. At TS1, three peroxyacid molecules are needed. At TS3, two or three peroxyacid molecules are needed. Elementary processes of the B−V reaction were determined by the use of the (acetone and (H−CO−OOH)$_n$, n = 3) system. Reactions of n = 2 and n = 4 were confirmed to be unfavorable. The formic-acid-catalyzed addition[14] (TS1 in Figure 3-2) leading to the Criegee intermediate is favorable. However, the catalyzed rearrangement (TS3 in Figure 3-6) is not as favorable as that of n = 3 (TS3 in Figure 1-6). Therefore, in the B−V reactions where TS3's are rate-determining, the carboxylic acid catalyst does not have a significant meaning. In contrast, when TS1 is rate-determining in our n = 3 model (e.g., Figure 7-1), the catalyst would work significantly (Figure 8-1). In the initial stage of the B−V reaction, there is no carboxylic acid and the path via TS1 and TS3 in Figure 7 is undergone. At the later stage, the product, the carboxylic acid, begins to be concerned with TS1 and the rate-determining step would be switched, TS1 → TS3. This seems to be an autocatalytic function of the carboxylic acid.

The geometries of TS1 and TS3 in the trimer (n = 3) participation are nearly insensitive to the substituent on the peroxyacid. TS1 or TS3 may be the rate-determining step because of the opposite character of TS1 and TS3. TS1 is enhanced by the electrophilic substrate, and TS3 is promoted by the nucleophilic migrating group.

New results obtained in this work are summarized.

(1) The uncatalyzed B−V reactions occur readily in the combination of a ketone and a trimer (n = 3) of peroxyacids. Three elementary processes (TS1, TS2, and TS3) are involved. The reaction model comes from structural requirement, in particular, the hydrogen-bond directionality. The requirement has not been considered so far.

(2) The reaction model for n = 3 gives a much smaller activation energy $\Delta G^{\ddagger}$ ~ 20 kcal/mol than those reported previously (e.g., $\Delta G^{\ddagger}$ (TS1) = 45.6 kcal/mol and $\Delta G^{\ddagger}$ (TS3) = 51.3 kcal/mol).[8f]

(16) Conversion of k_2 to the free activation energy (+23.09 kcal/mol) was carried out according to the Eyring equation, $k_2 = (k_B T/h)(RT/P)e^{-\Delta G^{\ddagger}/RT}$, where k_B = Boltsmann's constant = 1.381×10^{-23} J K^{-1}, h = Planck's constant = 6.626×10^{-34} J·s, T = 305 K, P = 1 atm, R = gas constant = 0.082 atm L mol^{-1} K^{-1} = 1.987 cal mol^{-1} K^{-1}, and k_2 = 4.53×10^{-3} L mol^{-1} s^{-1}. See, for example: Sana, M.; Leroy, G.; Villaveces, J. L. *Theor. Chim. Acta (Berlin)* **1984**, *65*, 109.

(3) The autocatalytic or the added catalytic ketone lowers the activation energy of TS1 significantly, which was reported before.[14] However, the subsequent processes (i.e., after the Criegee intermediate) have not been investigated. In this work, the entire processes have been revealed, and the role of the catalytic ketone is found to be limited to TS1.

(4) Generality of the requirement (1) has been confirmed by the use of various ketones and peroxyacids. As concluded in ref 2b, in the B−V reactions, several steps can be rate-determining depending on the reaction condition and reactants. The present calculations seem to have clarified first how the rate-determining step may be switched.

Supporting Information Available: Optimized geometries and reaction coordinate vectors corresponding to respective sole imaginary frequencies for TSs (Figures S1−S10) and the Cartesian coordinates of the optimized geometries of Figures 1−8 and S2-3. This material is available free of charge via the Internet at http://pubs.acs.org.

JO0626562